Journal of Photopolymer Science and Technology
Volume 20, Number 5 (2007) 707–717 © 2007 TAPJ

Double Exposure Materials: Simulation Study of Feasibility

Jeffrey Byers[1], Saul Lee[2], Kane Jen[2], Paul Zimmerman[1], Nicholas J. Turro[3], C. Grant Willson[2]

[1]*SEMATECH, 2706 Montopolis Drive, Austin, Texas 78741 USA*
[2]*Department of Chemical Engineering, University of Texas at Austin, Austin, Texas 78712*
[3]*Department of Chemistry, Columbia University*

Double patterning and double exposure techniques have been proposed as possible methods for reducing half pitch resolution below k_1=0.25. Both methods have the potential to reduce the theoretical lithographic half pitch to k_1=0.125. Double patterning is a process-intensive method that requires multiple coat, develop, and etch steps to achieve the low k_1 imaging. Double exposure processes have been proposed that do not require multiple coat, develop, or etch steps. Potentially, double exposure processes will have a lower cost of ownership that double patterning. However, double exposure materials have not yet been proven to work experimentally. Before applying significant effort to develop double exposure materials, their feasibility can be determined using rigorous simulation techniques. This work presents a feasibility study of four types of double exposure materials and their potential process windows.

Keywords: Immersion Lithography, Double Exposure, Double Patterning

1. Introduction

The trend in the continual miniaturization of microelectronic devices insists that the size of the functional features on these devices must also be reduce to sustain the desired performance efficiency while still reducing the cost per transistor. However, the photolithography industry has reached a critical point such that each reduction in feature size requires an exponential increase in technical development and committed resources. Each generation often requires new imaging tools, resist chemistries, etc. This disparity between a reduction in feature size and increase in cost will likely increase for future generations.

Resolution as determined by the half pitch critical dimension (CD) is limited by the Rayleigh equation

$$CD = \frac{k_1 \cdot \lambda}{NA},$$

where k_1 is the process aggressiveness factor, λ is the wavelength of the imaging tool, and NA is the numerical aperture of the imaging lenses and the optical properties of the imaged materials. To reduce the half pitch CD, the industry must reduce k_1 or λ, or increase NA. The theoretical minimum value for k_1 with a single exposure is 0.25, but the generally accepted manufacturability limit is 0.27. The current industry standard imaging tool has a wavelength of 193 nm. Future imaging tools are proposed to operate in the extreme ultra violet (EUV) range with a λ of 13.4 nm; however, EUV technology will most likely not be viable until after 2013. With water immersion lithography, the maximum achievable NA is approximately 1.35. Increasing the NA requires simultaneous development of a high index lens material along with high index fluids and high index resists. Without major breakthroughs in optical materials, NA will plateau near 1.35. Given these parameters, the current CD limit is approximately 38 nm half pitch.

The next generation of DRAM below 38 nm is to have a CD of 32 nm half pitch and will be produced in 2013 [1]. To enable lithography at sub-32 nm half pitch, the industry will need to consider alternative resolution enhancement technologies. A potential approach to meeting the resolution requirements involves the use of double exposure (DE) or double patterning (DP) within the existing imaging framework. Both DE and DP involve overlapping two staggered exposures with each exposure having twice the desired pitch to form the eventual pattern.

Double patterning is defined as a two exposure pass lithographic process that requires a chemical development of the photoresist layers and possibly an intermediate etch step. Either of these two processing approaches will require the removal of the wafer from the exposure tool chuck and loss of

Received May 31, 2007
Accepted June 18, 2007

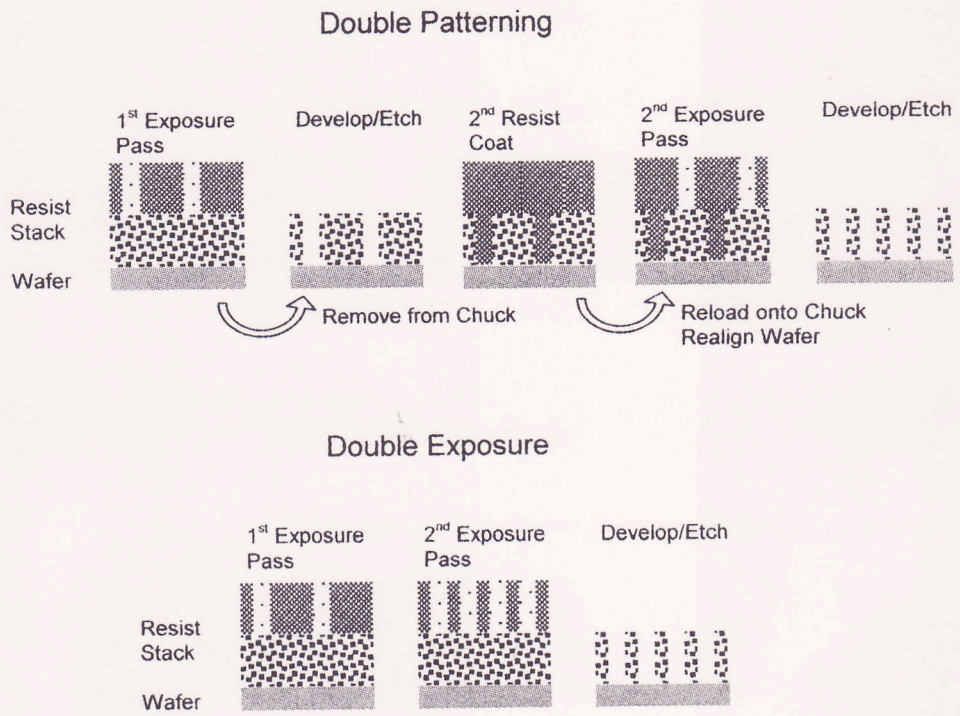

Figure 1 Comparison of the double patterning (development scheme shown) and double exposure processes

overlay registration. DE is defined as a two exposure pass lithographic process that does not require the removal of the wafer from the exposure tool chuck between passes. Double patterning and double exposure processes are illustrated in Figure 1.

The benefits of DE and DP principally include the ability to use existing exposure tools to print technology nodes below the NA limit for single exposure processes. This could mean a lower cost of ownership as these techniques can in principle be deployed without costly capital investment. However, the two exposure passes require doubling the number of masks and reduced throughput due to increased processing time. The process time is dramatically amplified in the DP process because it has more process steps than the DE process. In addition, removing the wafer from the wafer chuck between exposures poses severe overlay issues that may be difficult to overcome. The DE process introduces only an additional exposure pass, and since the wafer is not removed from the imaging tool between exposures, the overlay alignment issues are also minimized. The reduced cost of ownership of DE suggests that it would be the preferable technique for the industry.

The DE infrastructure is currently available on existing state-of-the-art exposure tools. DE is used to optimize imaging for certain features using techniques such as double dipole imaging [2]. However, imaging below a k_1 value of 0.25 with double exposure is impossible without the development of new materials. Dose reciprocity of conventional resists introduces a "memory" effect between exposures that prevents proper replication of the mask image into the resist. For example, the normalized aerial image intensities for the first exposure pass reaching the resist of equal lines and spaces can be described by the following,

$$I_{Pass1} = A\cos^2\left(\frac{\pi \cdot x}{pitch}\right) + B$$

where A is a constant describing the amplitude and B is the minimum image intensity. For the second exposure pass, the mask and, consequently, the aerial image are translated by half pitch and lead to the following intensity function

$$I_{Pass2} = A\cos^2\left(\frac{\pi \cdot x}{pitch} + \frac{\pi}{2}\right) + B$$

$$= A\sin^2\left(\frac{\pi \cdot x}{pitch}\right) + B$$

The dose reciprocity property of the resist causes a linear summation of the absorbed intensities from the two exposure passes. This leads to the following intensity function within the resist:

$$I_{Sum} = I_{Pass1} + I_{Pass2}$$
$$= A\cos^2\left(\frac{\pi \cdot x}{pitch}\right) + A\sin^2\left(\frac{\pi \cdot x}{pitch}\right) + 2B$$
$$= \text{a Constant!}$$

Therefore, the two individual mask images are not resolved when double exposed.

The resist system converts the separate light images, intensity versus position, into chemical images, chemical composition versus position. Mathematically, this conversion of the light image into a chemical image can be represented by a translation function (f). For standard resist systems, this translation function has the linear addition property:

$$f(I_{Pass1} + I_{Pass2}) = f(I_{Pass1}) + f(I_{Pass2})$$

This concept is illustrated in Figure 2.

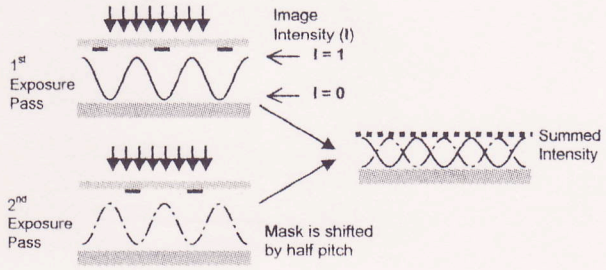

Figure 2 Summation of the intensity of the two exposure passes

Resolving the mask features requires a material with a nonlinear response in reciprocity to exposure dose such that

$$f(I_{Pass1} + I_{Pass2}) \neq f(I_{Pass1}) + f(I_{Pass2}),$$

and the resist memory behavior is minimized. Several material types have been proposed to enable a nonlinear response and are described in detail below.

2. Double Exposure Materials Description

Several materials types will theoretically permit double exposure pitch doubling. Four such material types are contrast enhancement layers (CELs), absorbance masking layers (AMLs), two-photon materials, and optical threshold materials. These four materials types are not the only possibilities but provide a reasonable range of chemistries to explore the feasibility of double exposure as a technology choice.

For simplicity, the resist translation functions given in this section are described in very simple terms. These empirical first order approximations allow for the demonstration of the desired material response for pitch doubling. However, the empirical first order approximations are not sufficient to predict the expected performance; consequently, theoretical image results were performed with more accurate models.

2.1. Contrast Enhancement Layer

Contrast enhancement layers (CELs) are materials that increase in transparency, or photobleach [3], when exposed to light. A CEL is normally applied directly on top of the resist layer. During the exposure, energy must first be devoted to photobleaching the CEL. Once the CEL is transparent, the energy is then able to reach the resist and initiate a solubility switch. Light can penetrate through the CEL only in regions where aerial image intensities are high (non-opaque regions on the mask); it cannot reach the resist in regions where aerial image intensities are lower (opaque regions on the mask). This introduces a nonlinear transfer of the applied aerial image into the photoresist and improves the resolution.

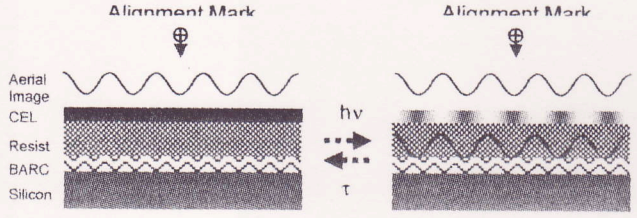

Figure 3: Schematic of contrast enhancement layer

CELs employ photochromics as the active component. Photochromics are materials that change optical density upon exposure to electromagnetic[4] or thermal radiation[5]. The change can be irreversible or reversible. In irreversible CELs[6], the material maintains transparency in the exposed regions while in

reversible CELs, the transparent regions are able to revert to full opacity after a delay or triggering event such as a flood exposure with light at an alternate wavelength. A delay range between 0.1 s to 60 s is ideal to fit within photolithography production specifications.

The light passing through the CEL is modified before forming the image in the resist. For simplicity, the image in resist can be described using a one-dimensional transmission model for the CEL with no scattering. This empirical first order approximation allows for the demonstration of dose reciprocity for double exposure but is not accurate enough for real image simulation. The theoretical image results were therefore performed with more accurate models. The first order CEL transmission function applied can be expressed as

$$f(I) \approx I \cdot e^{A \cdot C \cdot d \cdot I \cdot t} = I \cdot e^{\Delta \cdot I}$$

where A is the bleachable absorbance of the CEL, C is the bleaching rate, d is the thickness, and t is the exposure time. For reversible CEL materials, the DE aerial image is approximately

$$f(I_1) + f(I_2) \approx I_1 \cdot e^{\Delta \cdot I_1} + I_2 \cdot e^{\Delta \cdot I_2} \neq f(I_1 + I_2).$$

For irreversible CEL materials, the DE aerial image is approximately

$$f(I_1) + f(I_2) \approx I_1 \cdot e^{\Delta \cdot I_1} + I_2 \neq f(I_1 + I_2).$$

The equations show that reversible CELs have better image contrast than irreversible CELs because both exposure passes are enhanced by the material whereas only the first pass is fully enhanced in irreversible CELs. However, both CEL materials still show some nonlinear response to exposure energy.

For CELs to be used in current imaging tools, materials must be developed with photochromic chemistries that operate at a wavelength of 193 nm. The CEL must also be thin (< 100 nm) to minimize the effect on the depth of focus. The thinness requirement also stipulates that the material must be optically dense (ε/MW > 100 [7]) to be effective. The materials must also be able to be applied and removed without disturbing the underlying resist layers.

2.2. Absorbance Masking Layer

Absorbance masking layers (AMLs) are similar to CELs except that the materials are initially transparent and become opaque after exposure with radiation. The regions of high intensities from the first exposure pass turn the AML opaque which decreases the transmission of light from the second exposure pass into that region. This prevents the second exposure from overlapping the first exposure.

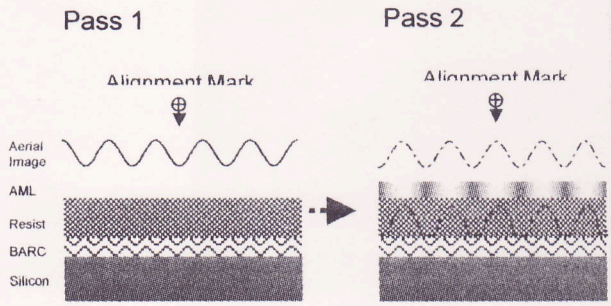

Figure 4 Schematic of absorbance masking layer

The AML translation function for double exposure is approximately

$$f(I_1) + f(I_2) \approx I_1 + I_2 \cdot e^{-\Delta \cdot I_1} \neq f(I_1 + I_2).$$

The first exposure pass has normal exposure characteristics since the AML layer is initially transparent everywhere. The additional negative sign in the enhancement transmission function from pass 2 indicates that the material becomes opaque after exposure to light during pass 1. Because the opacity distribution within the AML is dependent on the first exposure, I_1 is used in the enhancement transmission function for the second exposure.

Functioning AMLs do not yet exist and must be developed. The chemical viability of these systems is easily seen by considering the standard deprotection products of chemically amplified resists. In all chemically amplified resists, the deprotection reaction generates a double bond. These generated double bonds have the potential to increase the absorbance with each deprotection reaction. AML films can be designed using existing chemically amplified resist mechanisms.

Two obstacles for these systems are the need for a post-exposure bake to drive the reaction and the volatility of the deprotection products. Removing the wafer from the stepper to perform the post-exposure bake introduces a potential

overlay error. The volatility of the deprotection products reduces the effective absorbance gained and limits the masking efficiency.

Recent work on mass persistent resists may provide design pathways for overcoming the volatility issue [8]. Standard chemically amplified resists are driven to deprotection by the entropy gained from diffusion and evaporation of the deprotection products out of the resist film. Mass persistent resists use the lower enthalpy of the deprotected species to drive the reaction. The mechanism used by Frechet et al. generates a lower energy aromatic species that is tethered to the resist backbone. This approach should have the benefit of generating very large absorbance centers to achieve high masking efficiency.

2.3. Two-Photon Materials

Two-photon processes involve compounds that require absorption of two photons to induce a photochemical event such as the generation of a photoacid in a resist. The chemical reaction for a two-photon photoacid generator (PAG) is

$$\mathrm{PAG} + \mathrm{I}(h\upsilon) + \mathrm{I}(h\upsilon) \xrightarrow{\varphi} \mathrm{Acid},$$

where ϕ is the quantum efficiency. The probability of conversion is proportional to the light intensity squared and leads to a nonlinear response to exposure energy:

$$f(I) \approx I \cdot I .$$

The DE conversion is

$$f(I_1) + f(I_2) \approx I_1 \cdot I_1 + I_2 \cdot I_2 \neq f(I_1 + I_2).$$

Unlike the CEL and AML, two-photon materials are not enhancement layers that are applied onto resists to enhance resolution, but rather the nonlinear response is incorporated into the resist. This eliminates complexities introduced by the addition of an enhancement layer such as depth of focus and material compatibility.

Two-photon resist systems for microfabrication using laser writing systems have been developed[9]. These systems employ specially designed PAGs with high two-photon absorbance cross sections at visible wavelengths (λ>400 nm). The photogenerated acid can be used in either positive or negative tone resist systems. However, high efficiency two-photon PAGs have not yet been developed to work with 193 nm imaging light. The current two-photon PAG systems would require very large exposure intensity increases to be effective in projection optic processes.

2.4. Optical Threshold Materials

Optical threshold layers (OTLs) are materials that require the absorption of a threshold exposure dose to induce a photochemical event. Similar to two-photon materials, the exposure threshold gives the material a region of nonlinear response to exposure dose and allows OTLs to be used as double exposure resists. Resist memory effects are minimized because any dose absorbed below the threshold does not cause reactions to occur.

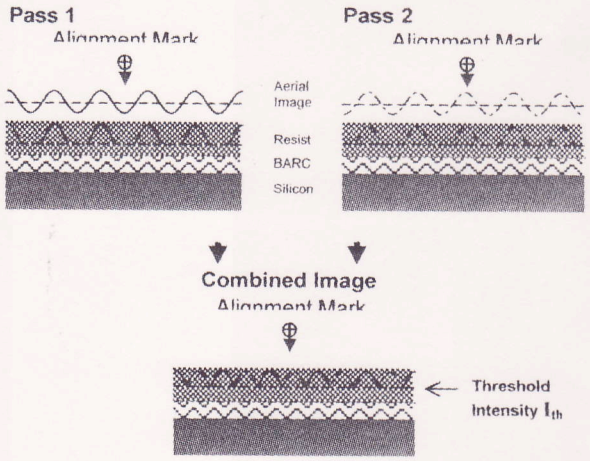

Figure 5 Schematic of the optical threshold layer

The conversion is proportional to the dose above the threshold I_{th} and is

$$f(I) \approx \max(I - I_{th}, 0),$$

where the "max" function has the following behavior:

$$\max(I - I_{th}, 0) = \begin{cases} 0, & I < I_{th} \\ I - I_{th}, & I \geq I_{th} \end{cases}.$$

Analogous thermal resist systems are already in use in the printing industry [10]. Thermal resists rely upon a thermal image instead of an optical image. The thermal image is derived from the absorbance of high intensity light images. Chapman et al. have investigated inorganic thermal resist systems [11] that use Bi/In bilayers as an etch masking layer for silicon. Chemical systems with similar properties for optical images have to be developed to use this technology with lithographic imaging systems.

3. Impact on Mask Design

The preliminary theoretical imaging studies show that DE with positive tone resists is a trench-based process. For a single exposure pass, positive tone resists should lead to line-based lithography where opaque regions on the mask produce lines in the resists plane after development while negative tone resists should lead to trench-based lithography where opaque regions on the mask produces trenches or spaces on the resist plane after development. The lines and spaces are transferred into the wafer with subsequent etch steps. The two processes are illustrated in Figure 6.

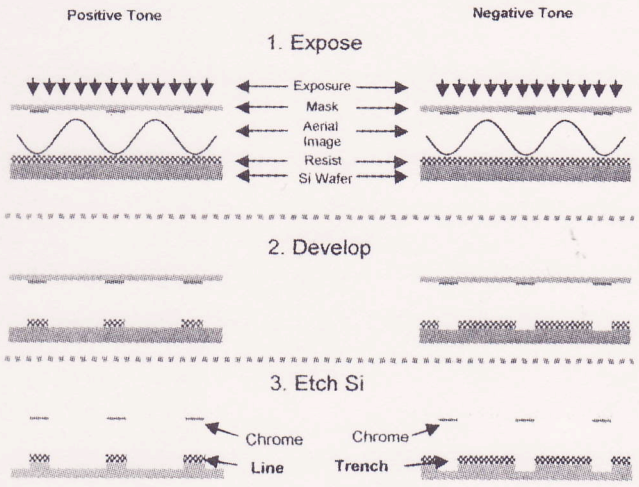

Figure 6 Line versus trench-based lithography

DE complicates the concept of mask tone because the lower intensity regions under the opaque regions in the first exposure pass may become the high intensity regions in the second exposure pass. The summation of the two exposure passes leads to an image in resist that develops away all regions under bright areas in either mask in positive tone resists. The resist features remain only in regions where both exposure masks have opaque regions. In negative tone resists, the regions under the bright regions in either mask would remain after development and form lines. This is illustrated in Figure 7 for positive tone resists.

Figure 7 shows two exposure passes and the combined energy distribution in the resist for an optical threshold system. Notice that in the "Combined Images," the peaks of high intensities correspond to the opaque region of the exposure mask from the other exposure. The valleys of the combined image correspond to regions where both masks have opaque regions either directly above or in close proximity. The final resist features are located at the valleys of the combined image.

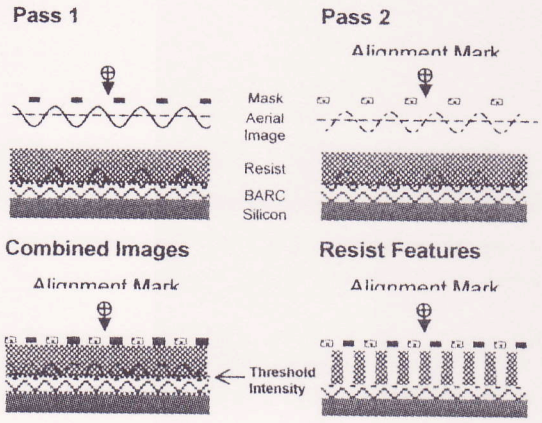

Figure 7 Double exposure effects on trench and line-based lithography

The characteristic of trench-based imaging has important implications for the design of masks for DE lithography and positive tone resists. The issues are different depending upon the class of the desired feature types. Dark field features should perform as expected with no consequences; however, care should be taken when patterning bright field features. The trench-based nature requires that mask design fracturing must be based on "trenches" or "spaces" surrounding gates. In other words, the size of a gate is no longer defined by the size of the corresponding opaque region on the mask and exposure dose but by the trenches around the gate and the mask registration errors between the two masks. The bright field design issues may be resolved by switching to negative tone double exposure resists.

To demonstrate the trench-based implications on mask fracturing, consider the mask fracturing required for printing contact holes (dark field features) and "5-bar" patterns (bright field features). The mask fracturings are shown in Figure 8 and Figure 9.

Figure 8 shows a target image of two columns of contact holes. The mask is fractured for DE such that the mask for the first exposure pass

contains contact holes in alternating diagonals and the mask for the second exposure pass contains the complementary contact holes not included in the first exposure pass. It should be noted that although the half pitch spacing between neighboring contact holes in each column and row can be theoretically reduced by a factor of two, the reduction is actually limited by the diagonal spacing between neighboring contact holes in each mask, which is constrained by the single exposure resolution limit. For printing contact holes, the pitch can be reduced by approximately 29% using double exposure.

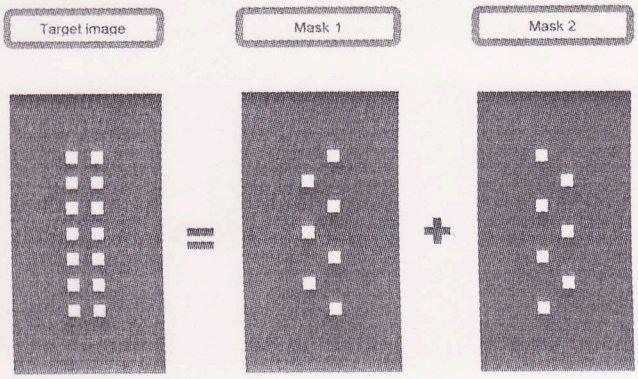

Figure 8 Mask fracturing scheme for contact holes

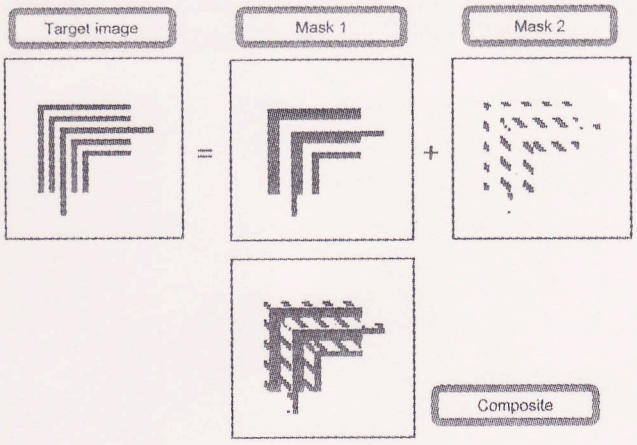

Figure 9 Mask fracturing scheme for 5-bar

Figure 9 shows the mask fracturing scheme for the 5-bar pattern. Since the lines are bright field features, the trench-based lithography requires that the mask be fractured such that the opaque areas are shifted so that lines in resist correspond to spaces in the masks. The centers of the non-opaque regions in each exposure pass combine to form the trenches on each side of a line. The edges of the non-opaque regions would receive lower doses in the resist and form the lines.

A full mask fracturing scheme for double exposure is beyond the scope of this work. The simple designs in Figure 8 and Figure 9 show that potential solutions exist for both dark field and bright field designs.

4. Simulations

The feasibility of the various proposed double exposure materials can be examined using simulation. Simulation allows the quick analysis of proposed material designs for potential performance without having to develop the materials. Using these results, the materials design efforts can be focused on those systems with the best theoretical chance of meeting the technical requirements of the semiconductor industry.

To correctly model the double exposure process, an in-house simulation was written. The simulator used the best known physical models for each proposed system. The basic assumption for this work was that the chosen double exposure resist systems would be based upon standard chemically amplified resists with only minor modifications. The basic models for chemically amplified resists are explained in detail elsewhere [12]. Likewise, the exact numerical methods for solving the explicit numerical equation are outside the scope of this paper and will be described elsewhere.

4.1. Model Description

The imaging optics project a grayscale image of the mask onto the silicon wafer. The image intensity is captured by the resist material during the exposure step. Because of the limitations of the projection optics, the image intensity is not an exact duplication of the mask design and the collected image energy must be accurately modeled. The details of calculating the image intensity in projection exposures can be found in several texts [12,13]. For imaging through CEL and AML, these standard models must be modified to account for the scattering effects from the CEL and AML layers. For this work, rigorous coupled wave analysis [14] (RCWA) was used to model the scattering of incident light through the CEL and AML layers.

The photobleaching of the CEL material is treated as a first order reaction between the photoactive compound and the light intensity:

$$A + \mathrm{I}(h\nu) \xrightarrow{\sigma_{CEL}} \mathrm{B} \xrightarrow{\tau_{CEL}} A$$

As the CEL material is exposed, the photoactive compound A absorbs light and is converted into a less absorbing material B with cross section σ_{CEL}. If the CEL material is reversible, then the less absorbing material reverts back to the absorbing material with some time constant τ_{CEL}. The rate equation for this reaction is given by

$$\frac{d[A]}{dt} = -\sigma_{CEL} \cdot I \cdot [A] + \frac{1}{\tau_{CEL}} \cdot [B]$$

Solutions to this rate equation are categorized by the value of the lifetime τ_{CEL}. Irreversible CEL materials ($\tau = \infty$) have the solution

$$f_A = \frac{A}{A_0} = e^{-\sigma_{CEL} \cdot \int_0^t I \cdot dt}$$

f_A is the fraction of starting material remaining in absorbing state A.

Reversible materials with lifetimes greater than the exposure time for each pass ($\tau >> t$) can also be simulated using this equation. For our simulations, the material is assumed to completely revert back to the absorbing form B at the beginning of the second exposure pass. This approximation can easily be removed by including the known delay between passes and the lifetime.

Reversible materials with fast reversibility ($\tau < t$) can be treated by numerical solution of the above rate equation or approximated using a steady state solution:

$$f_A = \frac{1}{1 + \sigma_{CEL} \cdot \tau_{CEL} \cdot I} = 1 - (\sigma_{CEL} \cdot \tau_{CEL}) \cdot I + \ldots$$

During exposure, the bleaching of the CEL material generates an optical grating. Subsequent incident light is scattered off this grating instead of simply traveling through the film stack as with uniform dielectric films.

In the RCWA model, the scattering effect is treated by assuming the complex refractive index, η, of the scattering layer is well represented by a Fourier expansion of the complex dielectric function ε:

$$\eta^2(x) = \varepsilon(x) = \sum_h \varepsilon_h \cdot e^{j \cdot \frac{2\pi \cdot h \cdot x}{pitch}}$$

In the CEL case, this is a good approximation since the bleaching function itself is a Fourier series arising from the nature of diffraction-limited imaging.

The refractive index at each point in the CEL material can be found, assuming an effective media approximation and the optical properties of the A and B compounds:

$$\eta_{CEL} = \eta_A \cdot f_A + \eta_B \cdot (1 - f_A)$$

The complete exposure model is constructed by combining the RCWA imaging model with one of the kinetic models for CEL bleaching described above. The exposure is broken up into many time steps. The image at each point in space is calculated at the beginning of each time step using the RCWA model. The concentration of optically active species f_A is then updated using the kinetic model assuming the image function is constant over the finite time step. This new optical profile is then fed into the next time iteration. Time stepping is continued until the desired exposure dose is reached.

To simulate the impact of absorbance masking layers, a simple model for generating absorbance was used. It was assumed that a first order model for conversion of light into absorbance centers would suffice. It was also assumed that a delay between the absorbance of light during the first pass and the generation of the absorbance centers was appropriate:

$$B + \mathrm{I}(h\nu) \xrightarrow{\sigma_{AML}} \mathrm{A}$$

$$f_{A,\mathrm{Pass2}} = 1 - e^{-\sigma_{AML} \cdot I_{\mathrm{Pass1}} \cdot Dose}$$

With this assumption, the first pass exposure condition was not modified from the standard exposure model. The creation of absorbance centers was then implemented between pass 1 and pass 2. Pass 2 must then be modeled just as the CEL materials by allowing the incident image to scatter off the AML gratings generated during pass 1. The RCWA model was used to generate the image in resist with AMLs during pass 2.

During exposure, the light image is captured by the resist material and converted through a photochemical reaction into a catalytic acid species.

The basic model for acid generation is a first order reaction between light and the photoacid generator (PAG). This is described schematically by

$$PAG + \mathrm{I}(h\nu) \xrightarrow{C} \mathrm{Acid}$$

where C is the rate constant for conversion. Under this first order assumption, the total yield of acid is a function of the integrated intensity or exposure dose.

$$[\mathrm{Acid}] = [\mathrm{PAG}] \cdot \left(1 - e^{-C \cdot \int \mathrm{I}\, dt}\right)$$
$$= [\mathrm{PAG}] \cdot \left(1 - e^{-C \cdot \mathrm{Dose} \cdot \mathrm{I}}\right)$$

For two photon materials, the acid conversion mechanism must be modified to include two photons for each conversion step:

$$PAG + 2 \cdot \mathrm{I}(h\nu) \xrightarrow{\sigma_2} \mathrm{Acid}\,.$$

This leads to an acid yield function that depends upon the integral of the instantaneous intensity squared:

$$[\mathrm{Acid}]_{2h\upsilon} = [\mathrm{PAG}] \cdot \left(1 - e^{-\sigma_2 \cdot \int \mathrm{I}^2 \cdot dt}\right) .$$

For Gaussian pulses with a pulse width τ_{FWHM} and laser rep rate f_{Hz}, the acid yield can be related to the square of the first order intensity function

$$[\mathrm{Acid}]_{2h\upsilon} = [\mathrm{PAG}] \cdot \left(1 - e^{-C_2 \cdot \mathrm{I}^2 \cdot Dose}\right)$$

where

$$C_2 = \frac{\sqrt{2\ln(2)}}{\sqrt{\pi}} \cdot \frac{\sigma_2}{\tau_{FWHM} \cdot f_{Hz}} .$$

The exposure model for the nonlinear optical threshold materials was set to a simple threshold function for acid generation. It is recognized that this type of model function is not an exact representation of potential chemistries but should provide some information about the expected performance of these systems:

$$[\mathrm{Acid}] = [\mathrm{PAG}] \cdot \left(1 - e^{-C \cdot \max\{\mathrm{Dose} \cdot \mathrm{I} - E_{th}, 0\}}\right)$$

During the post-exposure bake (PEB), the photogenerated acid molecules catalyze the deprotection of polymer sites to generate soluble species. The generally accepted kinetics for this system is described schematically by the set of reactions

$$M + \mathrm{Acid} \xrightarrow{k_a} S + \mathrm{Acid}$$

$$\mathrm{Acid} + Q \xrightarrow{k_Q} HQ$$

where M is the protected polymer site, S is the unprotected polymer site, Q is a base additive for quenching the catalyst, k_a is the amplification rate constant, and k_Q is the quenching rate constant. The solution of the concentration of protected and deprotected sites after the PEB step must be obtained numerically by solving the following set of differential equations:

$$\frac{d[M]}{dt} = -k_a \cdot [\mathrm{Acid}] \cdot [M]$$

$$\frac{d[\mathrm{Acid}]}{dt} = -k_Q \cdot [\mathrm{Acid}] \cdot [Q] + D_H \nabla^2 [\mathrm{Acid}]$$

$$\frac{d[Q]}{dt} = -k_Q \cdot [\mathrm{Acid}] \cdot [Q] + D_Q \nabla^2 [Q]$$

Included here, in addition to the rate constants given above, are the diffusion coefficients for the acid, D_H, and base quencher, D_Q, molecules.

For the simulations used in this work, a threshold development model was assumed. In this model, all locations with M concentrations above a certain threshold, m_{th}, are insoluble and remain after the develop step. All locations with M below the threshold level are completely removed during the develop step.

4.2. Simulation Conditions

To test the feasibility of these double exposure materials, the process windows for dense line space features were simulated using each of the four material types. A half pitch CD of 25 nm was targeted using a 1.2 NA water immersion exposure system. This is an effective k_1 of 0.155.

The illuminator chosen was an azimuthally polarized cross-quadrupole with σ_{center}= 0.8 and σ_{radius}= 0.15. The mask was 6% attenuated phase-shift 50 nm line/space patterns. The two masks were offset 50 nm between exposure passes. The stack was 75 nm of resist (n=1.69, α=1.2μm^{-1}) on 32 nm of a single layer bottom anti-reflective coating (BARC) (n=1.82, k=0.49) on top of silicon.

The resist simulations were based upon a typical 193 nm resist system. The baseline parameters are given in Table 1. When simulating the nonlinear double exposure materials, only the required parameters were changed. The

parameters for each double exposure material option are also listed in Table 1.

Table 1: Resist parameters used for simulations

Parameter	Value	Materials
C	0.0655	Baseline
[Q]/[PAG]	0.17	Baseline
D_H (nm2/s)	2.7	Baseline
D_Q (nm2/s)	1.9	Baseline
k_a	0.223	Baseline
k_Q	1000	Baseline
m_{th}	0.5	Baseline
C_2	0.0655	Two Photon
E_{th} (mJ/cm^2)	10	OTL
σ_{CEL} (cm^2/mJ)	0.21	Rev CEL
A_{CEL} (um^{-1})	30	Rev CEL
B_{CEL} (um^{-1})	0	Rev CEL

4.3. Results

Optical threshold layers, two-photon PAGs, and reversible CELs all yield process windows for sub-0.25 k_1 features when used in double exposure mode. The simulated Bossung plots (CD vs. focus for varying exposure dose) for these three systems are shown in Figure 10 through Figure 12. For comparison, the simulated Bossung plots for the line and trench-based conventional double patterning techniques are also shown in Figure 13 and Figure 14, respectively. Results for the nonreversible CEL and AML materials are not shown. These two materials did not show sufficient process windows for double patterning using the parameters chosen.

Analysis of these Bossung plots shows that the line-based double patterning technique yields the largest process window as given in Table 2. This is most likely because the resist parameters chosen are based upon a logic resist system that favors line imaging over trench imaging. When analyzing the relative merits of the double exposure materials, it is best to compare the obtained process windows with the trench-based double patterning results. All three DE materials show roughly half the depth of focus of the trench-based double exposure process. It is unclear at present if this can be improved by specifically optimizing the resist for double exposure. The optical threshold system singly showed comparable exposure latitude with the double patterning process.

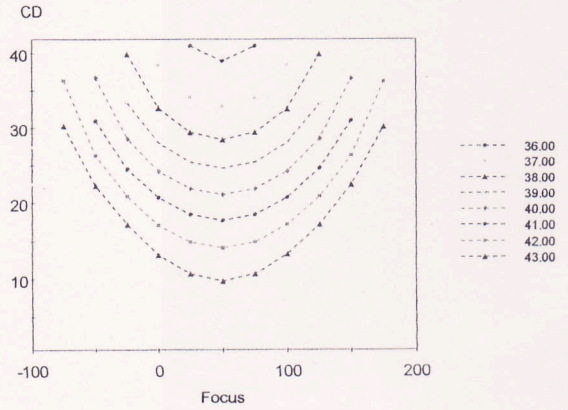

Figure 10 Bossung plot for 2 5 nm lines and spaces using the optical threshold layer double exposure system

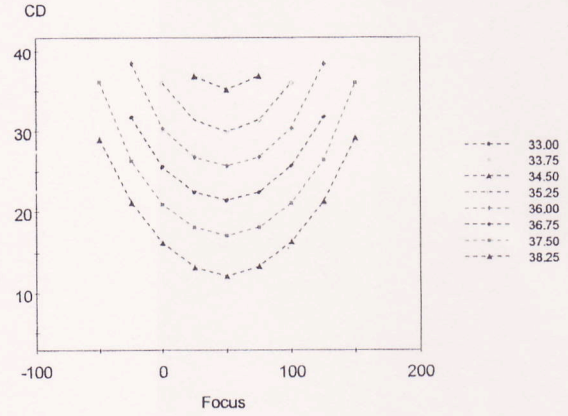

Figure 11 Bossung plot for 25 nm lines and spaces using the two-photon PAG double exposure system

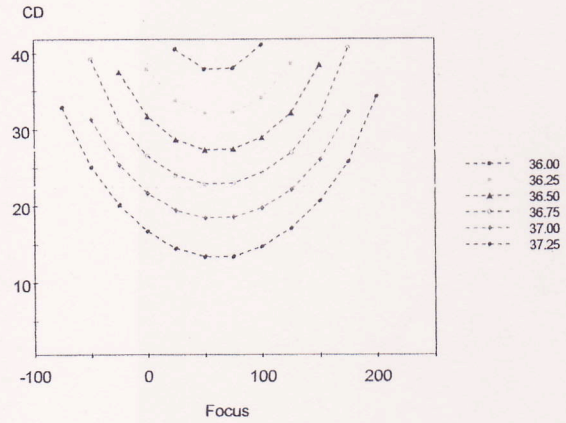

Figure 12 Bossung plot for 25 nm lines and spaces using the reversible CEL double exposure system

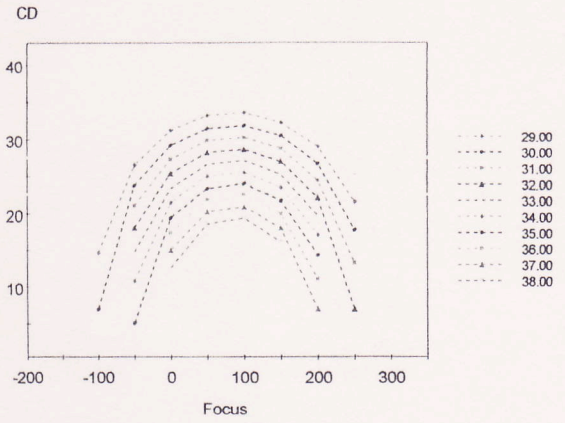

Figure 13 Bossung plot for 25 nm lines and spaces using line based double patterning

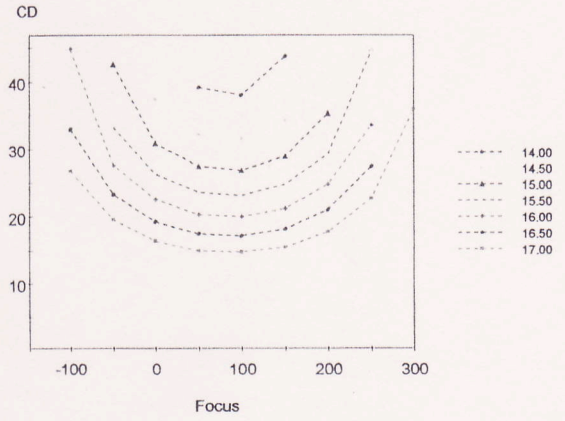

Figure 14 Bossung plot for 25 nm lines and spaces using trench based double patterning

Table 2 Depth of focus and exposure latitude for 25 nm lines and spaces

Process	DOF (nm)	EL (%)
Line Based DP	176	9.4
Trench Based DP	182	3.9
Optical Threshold Layer DE	110	3.18
Two-Photon DE	95	2.28
Reversible CEL DE	134	0.75

5. Conclusions

Double exposure is a potential resolution enhancement technique that will enable optical lithography at a k_1 less than 0.25 using current imaging tools. DE may also prove to be more cost-effective than double patterning. However, DE still requires the development and optimization of novel materials.

Of the proposed materials, our imaging studies showed that optical threshold layers have the most potential because of their high nonlinear response to dose and high image contrast. The possible chemistries for this approach still must be investigated. Two-photon PAG systems also show viability for double exposure. CEL materials show some promise but only for reversible systems. It is expected that any double exposure system must combine one or more of these individual nonlinear responses to have process windows competitive with double patterning.

References

1. 2006 Update: Lithography. International Technology Roadmap for Semiconductors [cited; Available from: http://www.itrs.net/Links/2006Update/2006UpdateFinal.htm.

2. S. D. Hsu, J. F. Chen, N. Cororan, W. T. Knose, D. J. Van Den Broeke, T. L. Laidig, K. E. Wampler, X. Shi, M.l Hsu, M. Eurlings, J. Finders, T. Chiou, R. J. Socha, W. Conley, Y. W. Hsieh, S. Tuan, and F. Hsieh., *Proc. SPIE* , **5040**, 2003, p. 215-231.

3. B.F. Griffing, and P.R. West, *Solid State Technology*, **28(5)** , 1985, p. 152-157.

4. M. M. Krayushkin, B. M. Uzhinov, A. Yu. Martynkin, D. L. Dzhavadov, M. A. Kalik, V. L. Ivanov, F. M. Stoyanovich, L. D. Uzhinova, and O. Yu. Zolotarskaya1, *International Journal of Photoenergy*. **1(3)**, 1999, p. 183-190.

5. R.S. Becker, and J. Michl, *Journal of the American Chemical Society*, **88(24)**, 1966, p. 5931-5933.

6 . B.D. Grant, et al., *Electron Devices, IEEE Transactions* , **28(11)**, 1981, p. 1300-1305.

7. P.R. West, G.C. Davis, and B.F. Griffing, *Journal of Imaging Science*, **30(2)**, 1986, p. 65-68.

8. J. M. Klopp, N. Bensel, Z. M. Fresco and J. M. J. Fréchet. *Chem.. Commun.*, 2002, p. 2956–2957.

9. S.M. Kuebler, et al, *Journal of Photochemistry and Photobiology A: Chemistry*, **158 (2-3)**, 2003, p. 163-170.

10. D. Gelbart, and V.A. Karasyuk, *Proc. SPIE*, **3676**, 1999. , p. 786-793.

11. G.H. Chapman, Y. Tu, and J. Peng, *Proc. SPIE*, **5039**, 2003, p. 472-484.

12. C. A. Mack, *Fundamental Principles of Optical Lithography: The Science of Microfabrication*, in press, John Wiley & Sons London, 2007.

13. D.G. Flagello, *High Numerical Aperture Imaging in Homogenious Thin Films*, Ph.D. Dissertation , University of Arizona, 1993.

14 . M. G. Moharam, Drew A. Pommet, Eric B. Grann ,and T. K. Gaylord, *J. Opt. Soc. Am. A*, **12(5)**, 1995, p. 1077-1086.